Journal of the Institute of Science and Engineering, Chuo University

Changes in the cell shape and actin organization accompanying primary ciliogenesis in *Xenopus* epithelial cells

Riho Ishigami and Takako Kato-Minoura

Abstract

Xenopus epithelial A6 cells produce primary cilia most readily when the confluent culture is serum-deprived, in contrast with various mammalian epithelial cells, which usually produce cilia in confluent cultures without serum starvation. Here, we observed A6 cells under the conditions that promote ciliogenesis, and found a few unusual features accompanying ciliogenesis including changes in cell shape and actin re-organization. Upon serum starvation, cells tended to reduce the area of attachment to the substratum and increase the height before ciliogenesis. Cells in highly ciliated areas formed thick actin bundles in their periphery. In addition, cells transiently formed a unique cone-shaped assembly of stress fibers, specifically in the basal region in the early phase of ciliogenesis. Although involvement of actin filaments in ciliogenesis has been widely recognized in recent studies, these actin structures have not been reported. Thus, ciliogenesis in A6 cells appears to reveal novel ciliogenesis-accompanying cellular changes that have been overlooked in studies using other cell lines.

1 Introduction

Primary cilia are non-motile, slender protrusions projecting from the apical surface of most kinds of non-proliferating cells in vertebrates [1]. Like motile cilia, primary cilia contain nine outer doublet microtubules and grow from the basal body. Unlike motile cilia, however, they lack the central pair of microtubules and dynein arms that are usually present in motile cilia. Primary cilia have chemo- and mechanoreceptors on their surface membrane and function as cellular antennas. Deficiency in cilia results in the development of compound diseases such as polycystic kidney disease, Bardet–Biedl syndrome, and Meckel syndrome [2, 3].

Despite increased medical interest in primary cilia, the mechanism that controls ciliogenesis is only partially understood[4, 5]. In this study, to explore the main cues for cilia production in epithelial sheets, we examined the process of ciliogenesis in A6 cells, a cell line derived from the *Xenopus* kidney epithelium. In contrast to other kidney epithelial cell lines such as MDCK (canine) or LLC-PK1 (porcine), the A6 cell line does not enter a quiescent state when cells reach confluence. Rather, after reaching confluence, the cells become detached from the substrate, form arches, and continue to grow. Under these conditions, the cells are not ciliated; they produce cilia only when the confluent culture is serum-starved. However, even after serum-starvation, the proportion of ciliated cells is as low as 30%, unlike mammalian epithelial cells which display ciliogenesis in almost 100% of cells in confluent cultures. Although the proportion of ciliated cells is low, A6 cells are useful for studying the conditions necessary for ciliogenesis because they need serum starvation for the initiation of ciliogenesis; therefore, we can compare cells under ciliogenic and non-ciliogenic conditions by supplying or depleting serum.

In the present study, we observed A6 cells under the conditions that promote ciliogenesis, paying

Biological Science Course, Graduate School of Science and Engineering, Chuo University, Kasuga, Bunkyo-ku, Tokyo, 112-8551, Japan; e-mail: minoura@bio.chuo-u.ac.jp

particular attention to the shape of the cells. A previous study with cultured human retinal cells showed that a smaller substrate area favored ciliogenesis [5]. Consistent with that study, we found that serum starvation induced a rapid decrease in the cell-adhesion area and an increase in the cell height.

In addition to the change in the cell shape, we observed characteristic changes in the actin cytoskeleton occurring before the production of cilia in A6 cells. These changes in actin structure may promote ciliogenesis partly by ensuring the cell to adopt a shape favorable for ciliogenesis.

2 Materials and methods

2.1 Cell culture

A6 cells were cultured in 50% Leibovitz's L15 medium (Thermo Fisher Scientific, Waltham, MA) supplemented with 10% (v/v) fetal bovine serum and 1% antibiotics (10,000 U/mL penicillin and 10,000 μg/mL streptomycin) at 22°C without CO_2 supplementation [6]. To induce the formation of primary cilia, A6 cells were cultured until confluence (4–6 days), at which point the medium was exchanged for fresh medium without fetal bovine serum. LLC-PK1 cells were cultured in 89% Dulbecco's modified Eagle's medium (Thermo Fisher Scientific) supplemented with 10% fetal bovine serum and 1% antibiotics. Cells were cultured at 37°C under an atmosphere containing 5% CO_2. To induce the formation of primary cilia, LLC-PK1 cells were cultured until confluence (4–6 days).

2.2 Immunofluorescence microscopy

Cells were cultured on coverslips, fixed with 10% formalin in phosphate-buffered saline (PBS), and demembranated with 0.1% Triton X-100 in PBS. After several washes with PBS, the coverslips were blocked with 1% bovine serum albumin in PBS. Primary antibodies (anti-tubulin DM1A [Santa Cruz Biotechnology Inc., Dallas, TX], anti-acetylated tubulin 6-11B-1 [Sigma-Aldrich, St. Louis, MO], anti-*Xenopus* myosin [7], and anti-vinculin [Sigma-Aldrich]) were diluted with the blocking solution and applied to the samples. After incubation for 1 h, the coverslips were washed with PBS, and the samples were reacted with secondary antibodies (Alexa488-labeled anti-mouse IgG, Alexa546-labeled anti-mouse IgG, and Alexa488-labeled anti-rabbit IgG [Thermo Fisher Scientific]). In some cases, rhodamine phalloidin, TO-PRO-3 (Thermo Fisher Scientific), Hoechst 33342, and Pyronin Y (Sigma-Aldrich) were used. After incubation for 1 h in the dark, the coverslips were washed with PBS and mounted on glass slides with Vectashield (Vector Laboratories, Burlingame, CA). Samples were examined by using a Zeiss 510 confocal laser-scanning microscope (Carl Zeiss, Oberkochen, Germany).

2.3 Measurement of cilia length and cell size

Ciliogenesis was induced by serum depletion. Samples were fixed immediately before serum depletion and at 1, 2, 5, 6, 7, and 8 days after serum depletion. Samples were then triple-stained with anti-tubulin (DM1A), phalloidin, and DAPI. Serial optical Z slices from the basal to the apical surface of each cell were acquired. 100 cells were randomly selected from each daily sample and the proportion of ciliated cells, judged from anti-tubulin staining, was counted. For the ciliary length, maximum intensity projection of the Z slices from those at the basal bodies to those at outside most of the cilia were created, and the ciliary length were measured. Cell height and the area of cell attachment to the substratum were determined from the phalloidin-stained actin boundary. Epithelial cells such as A6 have bundles of actin filaments just

beneath the cell membrane, and therefore we can regard rhodamine phalloidin-stained bundle images as cell borders. The area of the cell-attached substratum was easily measured as the area enclosed by the stained boundary. Z stacks were acquired from the basal to the apical surface of cells, and the slice where the peripheral F-actin was most clearly stained was selected and used (Fig. 1). Likewise, cell height was estimated from the distance between the apical-most and the basal-most slices by multiplying the single Z-slice thickness by the number of the slices where any F-actin signal was detected.

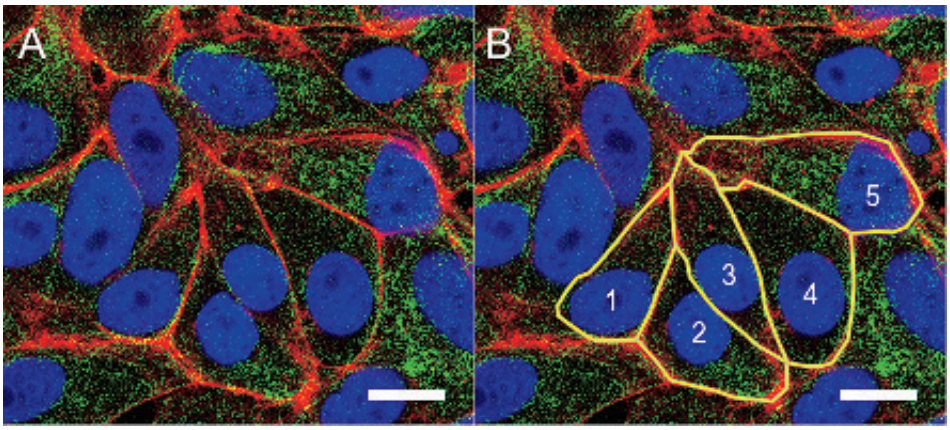

Figure 1. Method to estimate cell area by using rhodamine phalloidin staining. (A) Cells were fixed 6 days after serum depletion and then stained with rhodamine phalloidin, anti-tubulin (DM1A), and TO-PRO-3. (B) After capturing laser-scanning microscope images of the cells, actin filaments just below the cell membrane were traced, and the area of each cell (five cells are shown in the figure), which was defined as the area enclosed by the traced line, was calculated by using ImageJ software (National Institutes of Health, Maryland, US; https://imagej.nih.gov/ij/). Scale bars: 10 μm.

2.4 Live imaging

Expression vectors for mCherry–tubulin and Lifeact–enhanced green fluorescent protein (Lifeact–eGFP) were kindly supplied by Dr. Keiju Kamijo (Tohoku University, Sendai, Japan), and Dr. Kaoru Katoh (AIST, Tsukuba, Japan), respectively. A6 cells (100 μL;100 cells/μL in Opti-MEM [Thermo Fisher Scientific]) and 10 μg of CsCl-purified plasmid DNA were mixed, and DNA was introduced into the cells by means of electroporation with an NEPA21 electroporator (Nepa Gene Co., Ichikawa, Japan) under the following conditions: poring pulse: 2 × 2.5–5 ms/100–250 V, interval: 50 ms, voltage decay: 10%; transfer pulse: 5 × 50 ms/20 V, interval: 50 ms; and voltage decay, 40%. Cells were transferred to a glass-bottom dish and examined by using a Zeiss 510 confocal laser-scanning microscope.

2.5 Rac/CDC42-activator treatment

Subconfluent cells (approx. 60% confluent) were incubated with serum-depleted medium containing 0.25 U/mL of Rac/CDC42 activator II (CN02, Cytoskeleton, Denver, CO). When cells were cultivated for several days, the medium was refreshed daily. Statistical data comparison was performed using Student's *t* test.

3 Results

3.1 Ciliogenesis in A6 cells

Ciliogenesis was induced in A6 cells by omitting the serum from the culture medium after the cells had reached confluence. Aliquots of cells were fixed each day and stained for actin filaments, microtubules, and nuclei. Samples were examined under a laser-scanning microscope. At day 1 after serum depletion, less than 10% of the cells were ciliated (Fig. 2A). However, at day 2, the number of ciliated cells had increased to 30%. The proportion of ciliated cells then decreased until it reached 15% at day 8. Although each primary cilium observed in the cell images stained with tubulin antibody varied widely in length, the average length gradually increased from 4 μm at day 2 to 7 μm at day 7 (Fig. 2A).

3.2 Changes in cell shape after serum depletion

To test the hypothesis that spatial confinement promotes ciliogenesis [5], we measured the size of ciliated and non-ciliated cells after serum depletion. According to Pitaval et al. (2010), cells grown in a narrow space develop a cortical actin mesh that contracts and pushes up the apical cell membrane, producing a dome-like cell shape that favors ciliogenesis. If this is the case, we may assume that cell shape would change after serum depletion, a condition that would induce ciliogenesis in a subset of A6 cells. Consistent with this hypothesis, the average area of ciliated and non-ciliated cells, estimated in rhodamine phalloidin-stained cell images, decreased within a day (on day 0, approximately 550 μm^2 in non-ciliated cells; on day 1, approximately 370 μm^2 in ciliated cells, and approximately 330 μm^2 in non-ciliated cells, Fig. 2B). After that, the average area did not markedly change, remaining at approximately 380 μm^2. In addition, the average height of the cells increased (on day 0, approximately 3.3 μm in non-ciliated cells; on day 1, approximately 5.1 μm in ciliated cells, and approximately 5.5 μm in non-ciliated cells, Fig. 2C). Despite the marked decrease in the average area of the cells, the cell sheet remained confluent. This could be due partially to the presence of cells that had undergone cell division and/or to rearrangement of the cells, both of which are possible since A6 cells tend to detach from the substrate at confluence.

3.3 Change in actin-containing structures in the cell periphery under ciliogenic conditions

While examining the ciliogenic effects of cell shape, we noticed that some characteristic changes in actin organization had occurred during ciliogenesis. One such change, seen in both ciliated and non-ciliated cells under ciliogenic conditions, had occurred at the marginal region of the cells at the same height as the nuclear position; after serum starvation, thick actin bundles (width in Z direction, approx. 2 μm) were formed in cell sheets containing a high population (>30% in a frame) of ciliated cells (Fig. 3A), whereas only thin mesh-like actin structures (width in Z direction, approx. 0.6 μm) occurred in cell sheets containing a low population (<10% in a frame) of ciliated cells (Fig. 3B).

Thick actin bundles were seen only in highly ciliated regions, although they were present in both ciliated and non-ciliated cells in the same region of the cell sheet. From this observation, we hypothesized that the actin bundles promote ciliogenesis. To test this hypothesis, we examined the effect of an activator of Rac and CDC42, small G-proteins that promote actin polymerization and bundle formation at the cell periphery [8], on the ciliogenesis in non-confluent A6 cells. We used non-confluent cells wherein actin bundles were undeveloped, because confluent cells rapidly developed thick actin bundles after serum starvation, preventing clear evaluation of the activator effect on ciliogenesis. We thus applied

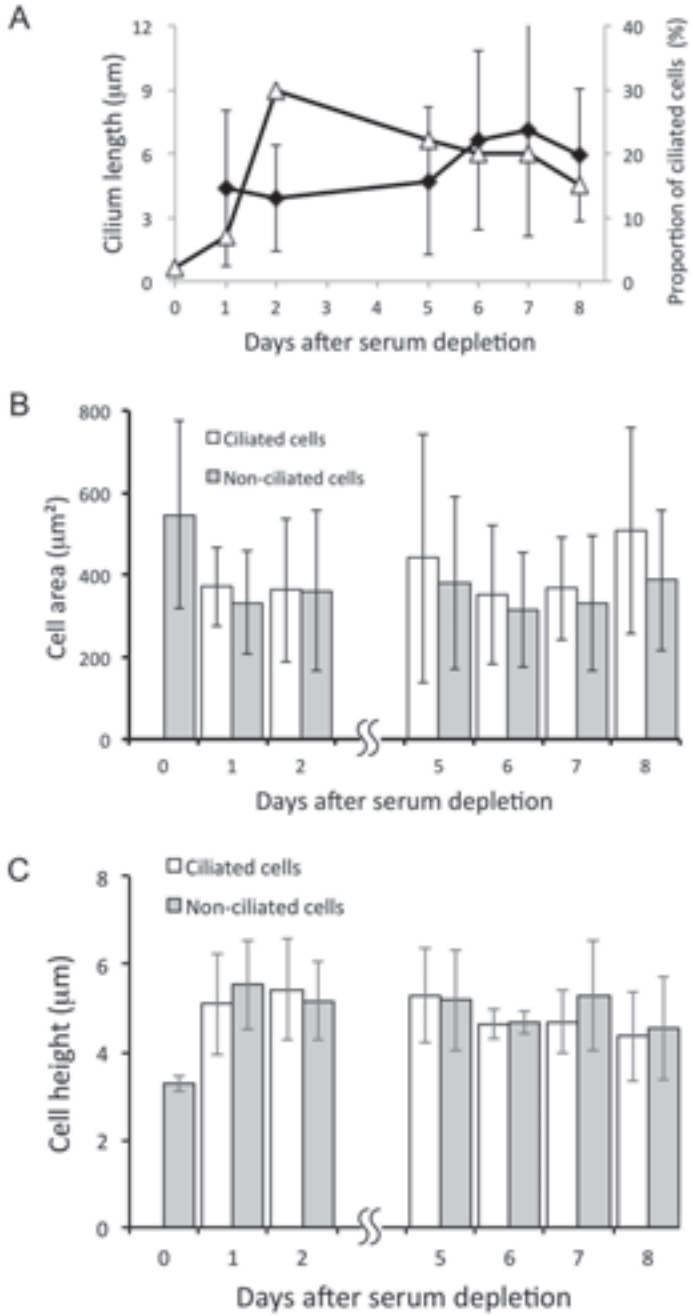

Figure 2. (A) Change in the proportion of ciliated cells (open triangles) and average length of primary cilia (solid rhombs) in A6 cells in ciliogenesis. Average area (B) and height (C) of ciliated and non-ciliated A6 cells. In each sample, ciliated cells and non-ciliated cells were randomly selected and their area (B) and height (C) were measured as in Materials and methods. Data were not collected at day 3 and 4. Error bars: 1 SD.

the activators to A6 cells at approximately 60% confluence after serum depletion. In this condition, the proportion of ciliated cells was as low as 3% (Fig. 4B). When the activator was applied, the peripheral actin bundles were more pronounced at day 3 (Fig. 4A). Furthermore, the proportion of ciliated cells increased to 15% in the activator-treated cells, whereas it did not increase from the initial 3% in the untreated cells (Fig. 4B). However, the final population of ciliated cells in the confluent cells did not appear to increase by treatment with the activator (data not shown).

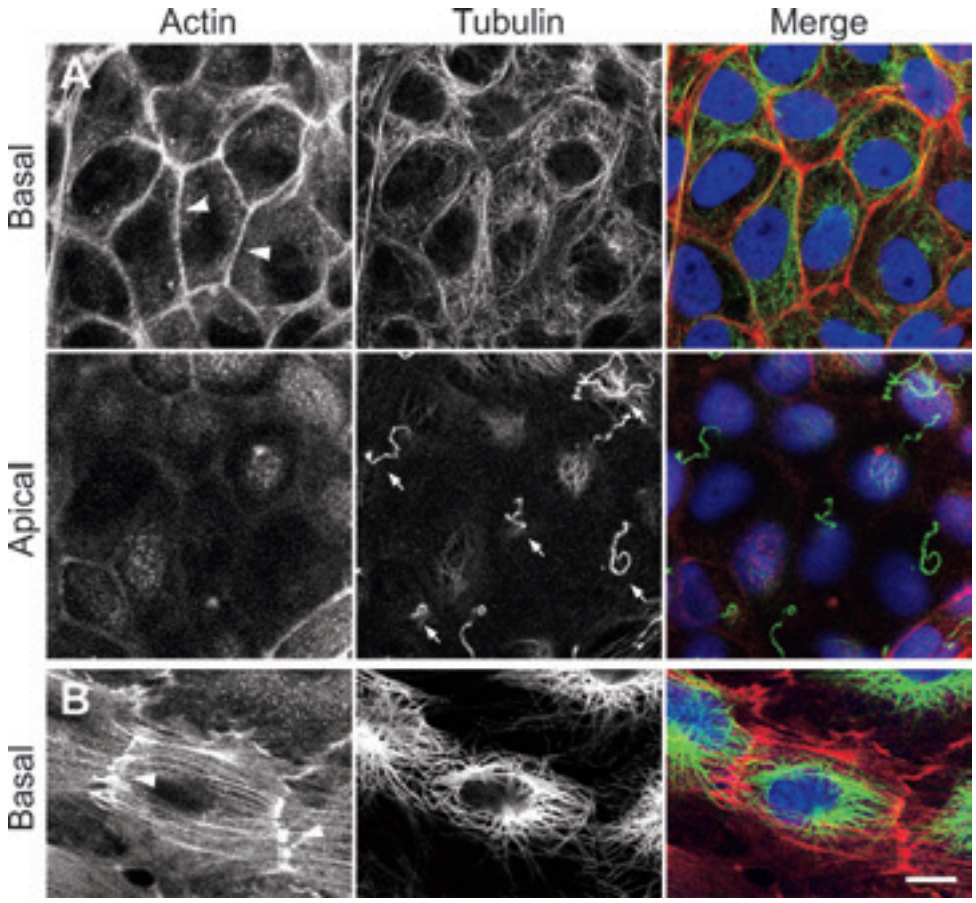

Figure 3. Ciliated and non-ciliated A6 cells have different actin structures at the cell periphery. Actin filaments and microtubules were stained with rhodamine phalloidin, DM1A antibody, and Alexa488 anti-mouse IgG antibody. (A) Ciliated cells 4 days after serum depletion. Serial optical Z slices (Z=1 to Z=8) from the basal to the apical surface of each cell were acquired. An average intensity projection of the slices (Z=4 and Z=5, total thickness: 2.0 μm) was created, which was approx. 2.5 μm above the substrate (upper panels). Thick actin bundles (arrowheads) were observed in this projection. Primary cilia (arrows, lower panels) were detected in an apical slice (Z=6, 4.0 μm above the substrate). (B) A non-ciliated cell 5 days after serum depletion. Serial optical Z slices (Z=1 to Z=30) from the basal to the apical surface of each cell were acquired, and an average intensity projection of the slices (Z=12 to Z=14, total thickness: 1.0 μm) was created. Thin mesh-like actin filaments (arrowheads) were observed at the cell periphery (2.2 μm above the substrate, which was at about the same height as in A). Blue signals in the merged images are nuclei stained with TO-PRO-3. Bar: 10 μm.

3.4 Appearance of a cone-like actin structure in the basal region of ciliogenic cells

We found another actin-containing structure that was specific to cells engaged in early ciliogenesis. It appeared transiently in the basal region of A6 cells, slightly before cilia were formed, and was a cone-shaped structure with the appearance of umbrella ribs (Fig. 5A). Upon anti-tubulin staining, every cell containing this structure displayed a strong tubulin signal localized in the apical region, which is indicative of the early phase of ciliogenesis. Time-lapse observation using an A6 cell line expressing the actin marker Lifeact showed that this cone-shaped actin structure formed approximately 1 h before the onset of ciliogenesis and disappeared within 1 to 2 h when the cilium fluorescence became stronger (Fig. 5B). Myosin was localized around the center of the structure (except for at the central focus), indicating that the structure was a type of contractile stress-fiber (Fig. 5C). Vinculin was localized at the tip of every actin fiber, indicating that the structure was supported by focal adhesions (Fig. 5D).

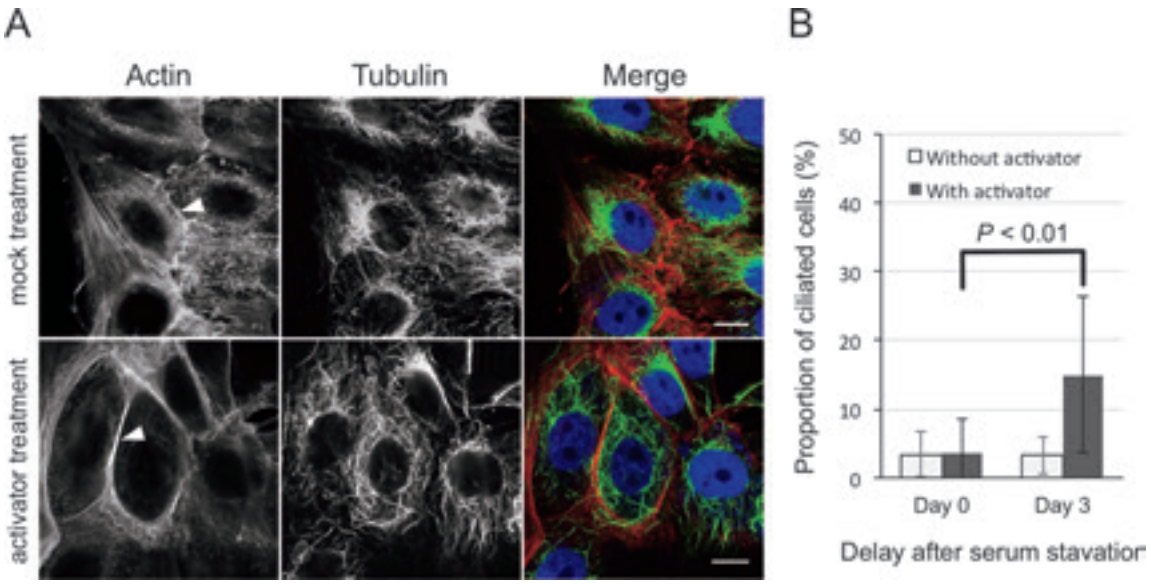

Figure 4. Effects of a Rac/CDC42 activator on actin rearrangement and ciliogenesis. (A) Effect on actin rearrangement. A6 cells at 60% confluence were serum depleted and treated with a Rac/CDC42 activator. The cells were fixed three days after the treatment with the activator and stained with rhodamine phalloidin, anti-acetylated-tubulin antibody, and Alexa488 anti-mouse IgG antibody. In mock-treated cells, actin filaments in the cell periphery were thin and dispersed (arrowhead, upper panels). In activator-treated cells, thick actin bundles appeared in the same region of the cell periphery in which the thin actin filaments were observed in the mock-treated cells (arrowhead, lower panel). Blue signals in the merged images are nuclei stained with TO-PRO-3. Bars: 10 μm. (B) Effect on ciliogenesis. The proportion of ciliated cells was counted in anti-tubulin stained images. Error bars: 1 SD. Statistical significance was determined by using the unpaired Student's *t*-test.

4 Discussion

In this study, we examined the cell shape in cultured *Xenopus* A6 epithelial cells under ciliogenic conditions. About 30% of the A6 cells became ciliated after reaching confluence and being serum-starved (Fig. 2A). After two days of serum depletion, the proportion of ciliated cells gradually decreased while the ciliary length increased only modestly, indicating that the state characterized by the occurrence of a small fraction of cells having 4-7 μm long cilia is the fully differentiated state of A6 cells within an epithelial sheet. In addition, within 1 day of serum depletion, the average cell area decreased and average cell height increased (Fig. 2B and C). Since ciliogenesis also took place shortly after serum depletion, these changes in cell area and height likely are critical cues for the induction of A6 ciliogenesis. This is consistent with the results of a previous study [5] that showed that non-ciliated cells grown on a large substrate (approx. 3000 μm^2) became ciliated when transferred to a smaller substrate (approx. 750 μm^2). Thus, alteration of cell shape may be an important factor for the onset of ciliogenesis. Pitaval et al. (2010) suggest that, in cells placed in narrower spaces, basal bodies migrate to the apical region, which promotes ciliogenesis. However, only 30% of the cells became ciliated even though all the cells changed shape after serum depletion. This indicates that other factors must exist that control ciliogenesis in this cell line.

We also found that characteristic changes in the actin structure occurred prior to ciliogenesis in the A6 cells. One change was the appearance of thick actin bundles in the marginal region of the cells (Fig. 3B). Although such bundles were observed in both ciliated and non-ciliated cells, they are apparently crucial for ciliogenesis because they appeared only in highly ciliated cell sheets under conditions that favored ciliogenesis. In fact, we found that, in serum-starved A6 cells at 60% confluence, stimulation of bundle

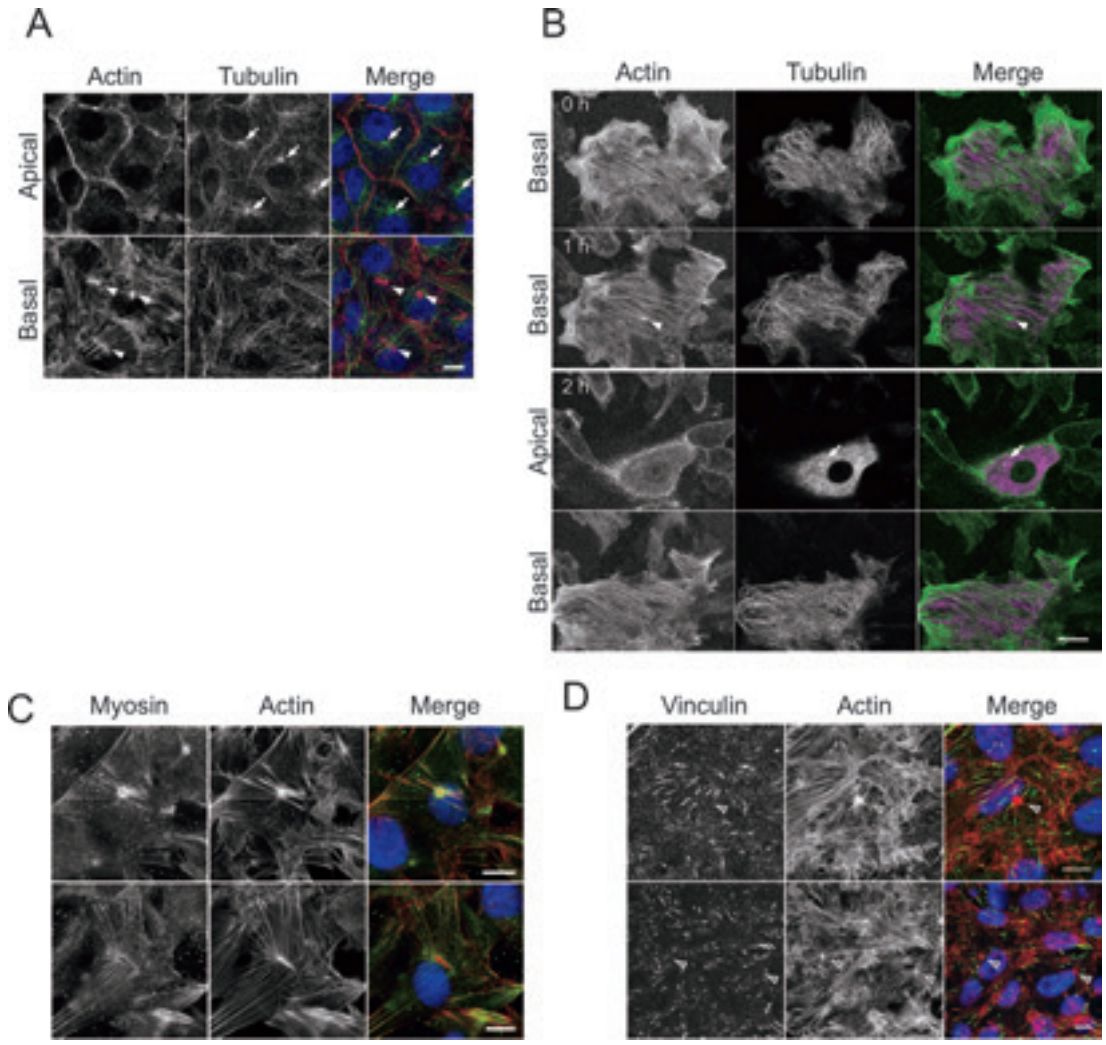

Figure 5. Cone-shaped actin structures in the basal region of A6 cells appeared just before ciliogenesis. (A) A6 cells under ciliogenic conditions were fixed and stained with rhodamine phalloidin, anti-tubulin antibody (DM1A), and Alexa488 anti-mouse IgG antibody. A Z stack from the apical to the basal surface of each cell was acquired. Cone-shaped actin structures (arrowheads) were observed in a basal slice (0.8 μm above the substrate). In an apical slice (1.8 μm above the substrate), strong anti-tubulin–stained dots (arrows) were observed near the nuclei (blue signal in merged images), indicating that these cells were in the process of early ciliogenesis. Bar: 10 μm. (B) Observation of actin filaments and microtubules over time. A6 cells co-expressing Lifeact–eGFP and mCherry-tubulin were observed. Bar: 20 μm. (C) Myosin localized at the center of the cone structure. Two examples of actin cone structures stained with rhodamine phalloidin, anti-*Xenopus* myosin antibody, and Alexa488 anti-rabbit IgG antibody. Blue signals in the merged images are nuclei-stained with TO-PRO-3. Bars: 10 μm. (D) Vinculin was localized at the tip of each astral actin fiber (arrowheads). Bars: 10 μm.

formation by administration of a Rac/CDC42 activator significantly increased the proportion of ciliated cells from 3% to 15% ($P < 0.01$; Fig. 4B). However, we did not see a significant increase in the percentage of ciliated cells in serum-starved, confluent cells with activator treatment (data not shown); therefore, the final rate of ciliated cells in the fully differentiated stage may be controlled by other developmental factors. The relationship between the development of thick actin bundles and appearance of ciliated cells remains to be explored further.

Another change observed in actin organization in ciliogenic cells was the transient formation of a cone-shaped, umbrella-rib-like fibers near the basal side of the cells (Fig. 5A). These fibers were composed of radially arranged actin bundles, the distal tips of which were linked with the focal adhesions (Fig. 5D).

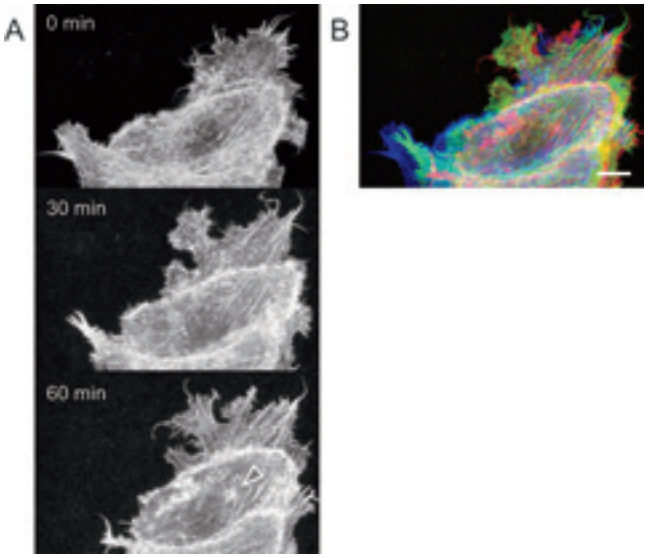

Figure 6. (A) Time-lapse observation of actin filaments in an A6 cell expressing Lifeact–eGFP. Arrowhead indicates a cone-like structure appearing 60 min after the onset of observation (B) Overlaid image of the three frames presented in (A). Images at time 0, 30 min, and 60 min were colored in blue, green and red, respectively. Bar: 20 μm.

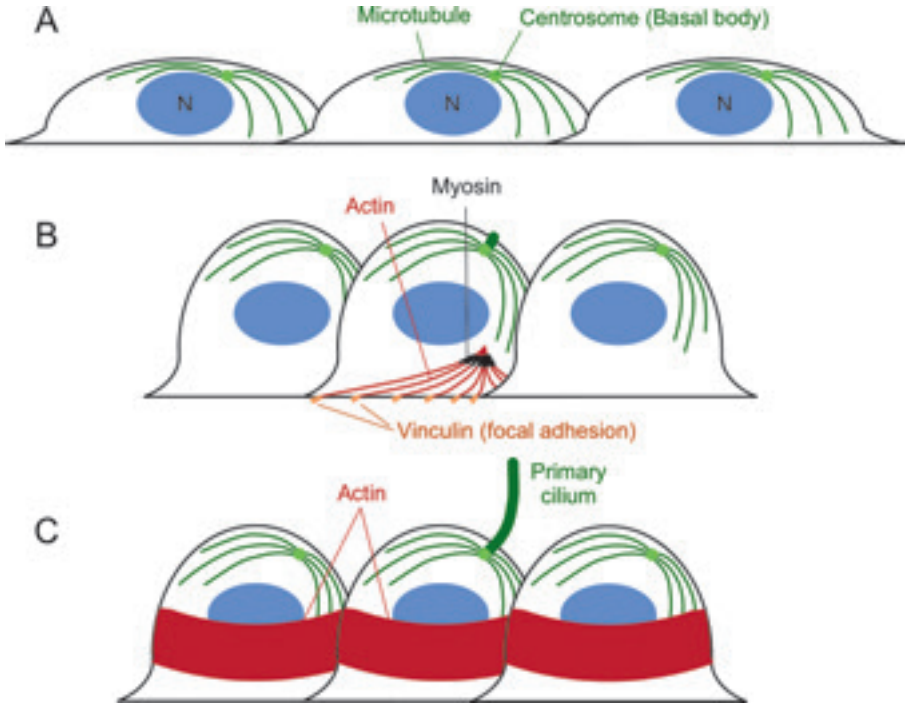

Figure 7. Model depicting the change in actin organization during A6 ciliogenesis. (A) Before ciliogenesis. No noticeable distinct actin structures are present, and the centrosome is localized near the nucleus (N). (B) After serum depletion, cells decrease their area of substrate attachment and increase their height. At the same time, the centrosome moves to the cortex and starts ciliogenesis. In a subset of cells that produce primary cilia, a contractile actin cone structure appears near the basal surface of the cell. Focal adhesions support these actin cones. (C) Over time, thick actin bundles develop at the cell margin and a cone structure disappears. These actin bundles produce a force directed to the cell center that supports the cell shape. This promotes formation of a cellular configuration that helps the basal body function as the base for a primary cilium.

Myosin II was localized around the center of this structure, indicating that this was a kind of contractile stress fiber (Fig. 5C). The myosin II signal was not present at the very center of the structure but was localized away from the center in a doughnut-like distribution. Although we do not understand the exact function of this unique structure in ciliogenesis, this myosin II localization suggests that this structure may produce radial tension that deforms the cell. In fact, Lifeact-labeled actin filaments forming this kind of radial fiber were sometimes observed at the cell base, and those cells gradually contracted toward their center (Fig. 6). Thus, we propose that these actin structures produce an inward force that drives ciliogenesis by both reinforcing the "heaped" cell shape induced by serum depletion and supporting the basal bodies (Fig. 7).

Various previous studies have indicated the importance of the actin cytoskeleton in ciliogenesis; rearrangement of the apical actin network coordinates cellular polarization, directs basal bodies to the apical surface, and provides membrane and ciliary components [9-13]. The actin structures observed in the present study were formed near the basal part of the cell, and therefore must differ in function from the previously studied actin structures formed just beneath the apical membrane. The actin structures observed in the present study did not appear to have any specific link to the basal bodies. Therefore, it seems unlikely that these actin structures directly promote the ciliogenic activity of basal bodies; rather it appears that they are important for maintaining the whole cell architecture, including maintenance of the reduced cell area and increased cell height brought about by serum starvation (Fig. 2). Elucidation of the function of these actin structures in ciliogenesis is an important subject for future studies.

5 Acknowledgements

The authors thank Dr. Sawako Yamashiro (Kyoto University) for her valuable discussions, Dr. Yoshiro Yajima (University of Tokyo) for his instruction on statistical analyses, and Dr. Ritsu Kamiya for his critical reading of the manuscript. This work was supported by the Joint Research Grant (Class 1) from The Institute of Science and Engineering, Chuo University.

6 References

[1] G.J. Pazour, G.B. Witman, The vertebrate primary cilium is a sensory organelle, Curr. Opin. Cell Biol. 15 (2003) 105-110.

[2] V. Singla, J.F. Reiter, The primary cilium as the cell's antenna: signaling at a sensory organelle, Science 313 (2006) 629-633.

[3] E.M. Valente, R.O. Rosti, E. Gibbs, J.G. Gleeson, Primary cilia in neurodevelopmental disorders, Nat Rev Neurol 10 (2014) 27-36.

[4] R.W. Tucker, A.B. Pardee, K. Fujiwara, Centriole ciliation is related to quiescence and DNA synthesis in 3T3 cells, Cell 17 (1979) 527-535.

[5] A. Pitaval, Q. Tseng, M. Bornens, M. Thery, Cell shape and contractility regulate ciliogenesis in cell cycle-arrested cells, J. Cell Biol. 191 (2010) 303-312.

[6] S. Yamashiro, T. Noguchi, I. Mabuchi, Localization of two IQGAPs in cultured cells and early

embryos of *Xenopus laevis*, Cell Motil. Cytoskel. 55 (2003) 36-50.

[7] T. Noguchi, I. Mabuchi, Reorganization of actin cytoskeleton at the growing end of the cleavage furrow of *Xenopus* egg during cytokinesis, J. Cell Sci. 114 (2001) 401-412.

[8] C.D. Nobes, A. Hall, Rho, rac, and cdc42 GTPases regulate the assembly of multimolecular focal complexes associated with actin stress fibers, lamellipodia, and filopodia, Cell 81 (1995) 53-62.

[9] I. Antoniades, P. Stylianou, P.A. Skourides, Making the connection: ciliary adhesion complexes anchor basal bodies to the actin cytoskeleton, Dev Cell 28 (2014) 70-80.

[10] J. Kim, J.E. Lee, S. Heynen-Genel, E. Suyama, K. Ono, K. Lee, T. Ideker, P. Aza-Blanc, J.G. Gleeson, Functional genomic screen for modulators of ciliogenesis and cilium length, Nature 464 (2010) 1048-1051.

[11] X. Yan, X. Zhu, Branched F-actin as a negative regulator of cilia formation, Exp. Cell Res. 319 (2013) 147-151.

[12] Y. Rao, R. Hao, B. Wang, T.P. Yao, A *Mec17-myosin II* effector axis coordinates microtubule acetylation and actin dynamics to control primary cilium biogenesis, PLoS One 9 (2014) e114087.

[13] M.E. Werner, P. Hwang, F. Huisman, P. Taborek, C.C. Yu, B.J. Mitchell, Actin and microtubules drive differential aspects of planar cell polarity in multiciliated cells, J. Cell Biol. 195 (2011) 19-26.